Nano-encapsulation Method for High Selectivity Sensing of Hydrogen Peroxide inside Live Cells

Gwangseong Kim[†,‡], **Yong-Eun Koo Lee**[‡], **Hao Xu**[‡], **Martin A. Philbert**[§], and **Raoul Kopelman**[*,†,‡]

[†] Department of Biomedical Engineering, University of Michigan, Ann Arbor, Michigan

[‡] Department of Chemistry, University of Michigan, Ann Arbor, Michigan

[§] Department of Environmental Health Sciences, University of Michigan, Ann Arbor, Michigan

Abstract
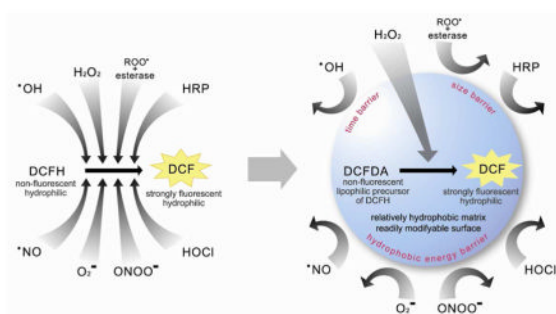
Reactive oxygen species (ROS) are ubiquitous in life and death processes of cells[1], with a major role played by the most stable ROS, hydrogen peroxide (H_2O_2). However, the study of H_2O_2 in live cells has been hampered by the absence of selective probes. Described here is a novel nanoprobe ("nanoPEBBLE") with dramatically improved H_2O_2 selectivity. The traditional molecular probe, 2′, 7′-dichlorofluorescin (DCFH), which is also sensitive to most other ROS, was empowered with high selectivity by a nanomatrix that blocks the interference from all other ROS (hydroxyl radical, superoxide, nitric oxide, peroxynitrite, hypochlorous acid and alkylperoxyl radical), as well as from enzymes such as peroxidases. The blocking is based on the combination of multiple exclusion principles: time barrier, hydrophobic energy barrier, size barrier. However, H_2O_2 sensitivity is maintained down to low nM. The surface of the nanoprobe was engineered to address biological applications, and the power of this new nanoPEBBLE is demonstrated by its use on RAW264.7 murine macrophages. These nanoprobes may provide a powerful chemical detection/imaging tool for investigating biological mechanisms related to H_2O_2, or other species, with high spatial and temporal resolution.

H_2O_2 is a key player in intracellular signaling[2,3], host defense and phagocytosis[4,5,6,7], wound detection and healing[8], as well as in the initiation of several pathophysiological cascades that terminate in cell death or adaptation[9,10]. H_2O_2 is a by-product from other ROS related reactions, such as the dismutation of the superoxide radical anion (O_2^-) under the mediation of superoxide dismutase. It is also a common precursor for the further generation of other, more

damaging, ROS, such as hydroxyl radical ($\cdot$OH), hypochlorous acid (HOCl) and peroxynitrite (ONOO$^-$)[11,12,13]. H_2O_2 is a relatively stable ROS, amenable to measurement, and, as such, has drawn much interest. However, specific and readily deployable tools for reliable and precise physiological/intracellular measurements of H_2O_2 are still lacking.

Many ROS sensitive molecular probes have severe limitations, such as poor selectivity and instability, thus often leading to spontaneous oxidation (Supplementary figure 1)[14,15]. Further complications, such as the inability of specific probes to permeate biological membranes and the potential interference by unwanted enzymatic reactions, need to be considered for quantitative measurements under physiological conditions. DCFH (2′,7′-dichlorofluorescin) dye is highly sensitive and is one of the most widely used probes for the detection of ROS and oxidative stress in biolological systems[16,17,18]. For intracellular measurements, the non-fluorescent and lipophilic precursor molecule, DCFDA (2′,7′-dichlorofluorescin diacetate), is used to freely pass into the plasma membrane. The DCFDA dye then converts into the hydrophilic DCFH, inside the cell, by losing two acetate groups due to esterase activity. DCFH can readily generate the strongly fluorescent and hydrophilic product, 2′,7′-dichlorofluorescein (DCF), upon oxidation by ROS generated inside of cells. Although this dye has often been used to monitor H_2O_2, its poor selectivity strictly limits the utility of the measurements to systems that are relatively free from interferences. Furthermore, its pH sensitivity is a well known drawback[19]. Also, its use often depends on a catalytic activity of peroxidases, which can complete the transition to DCF even without ROS, and thus hurting the accuracy of detection[16,17]. Those limitations hamper its application in most biological situations.

Nanoparticle platforms provide a working solution that addresses many of the problems identified above. Our group has developed nanoparticle based biosensors, termed PEBBLEs (Photonic Explorers for Biomedical uses with Biologically Localized Embedding)[20,21,22], for the intracellular detection of a large number of biologically important analytes. NanoPEBBLE sensors provide several important advantages over conventional sensors such as molecular probes: minimal physical/chemical invasiveness, minimal interference between probe and cell ingredients, a wider choice of probe materials, synergistic detection schemes, biological targeting, autofluorescence background suppression, and a ratiometric measurement capability[23]. Here we describe an added benefit: induced selectivity.

Recently, several attempts to improve H_2O_2 detection have been reported, based on either chemical modification of the ROS probes or nanoparticle-based approaches. Gong *et al.*[24], Dickinson *et al.*[25], Maeda *et al.*[26] and Setsukinai *et al.*[14] suggested various chemical derivatizations of DCFDA. Lee *et al.*[27,28] developed a polymer nanoparticle based on a peroxalate chemiluminescence (POCL)[29], which is a well known chemiluminence technique for H_2O_2 detection. Kim *et al.*[30] and Poulson *et al.*[31] reported nanoparticles that embed peroxidases in hydrophilic polymer matrices. Both approaches are based on the selectivity of peroxidases and their catalytic effect. In spite of these advances, some limitations still remain, such as imperfect selectivity, interferences by enzymes and by non-ROS chemicals, unverified particle biocompatibility, leaching from particles, and insufficient dynamic ranges of detection.

In contrast, the approach given below utilizes the nanoparticle as a screening device that empowers high H_2O_2 selectivity to an otherwise non-selective probe, DCFH. Such induced selectivity can be achieved by a delicate complimentarity of properties between the nanoparticle matrix and the embedded molecular probe (Scheme 1). In addition, this nanoprobe has other typical benefits of nanoPEBBLEs, such as biocompatibility, protection of content and targeting capability.

Ormosil nanoplatforms, which are bio-inert, relatively hydrophobic but still water-suspendable, with a 100 nm size (Supplementary figure 2), were synthesized by a previously

described method[32,33]. The nanoparticle surface is readily modifiable by amine functionalization (resulting in about 20 mV of zeta potential, indicating a positive surface charge). DCFDA was loaded into preformed Ormosil particles by a solvent displacement technique (Supplementary figure 3)[34,35], wherein hydrophobic dye molecules and particles are dissolved in a volatile organic solvent first, mixed with aqueous media and then the solvent is evaporated. The resulting nanoparticle retains the dye molecule in its inactive/lypophilic form, DCFDA. We discovered that the DCFDA dye shows H_2O_2 sensitivity without conversion to the activated hydrophilic intermediate (DCFH), in contrast to previous reports[16–18] (Table 1 and Supplementary figure 4). The DCFDA nanoprobes (0.1 mg/mL) displayed an increase in fluorescence intensity over time, upon addition of H_2O_2. The fluorescence intensity value reached a plateau after very long time (supplementary figure 5). The plateau value varied monotonously with H_2O_2 concentration. The early-time rate of fluorescence generation also depends on H_2O_2 concentration, as demonstrated in Table 1. The nanoprobes detected H_2O_2 over a concentration range of 10 – 100 μM—a significantly wider detectable range than previous probes'[27,30,31]. These DCFDA nanoprobes showed negligible dye leaching, confirming that the H_2O_2 response was not from released dye molecules in solution (Figure 1).

The H_2O_2 selectivity of the DCFDA nanoprobe and the DCFDA free dye has been examined by monitoring the change in fluorescence intensity upon exposure to various ROS interferents, such as ˙OH, O_2^-, ˙NO, ONOO⁻, HOCl, and ROO˙ (alkylperoxyl radical) (Table 2). The DCFDA free dye was prepared by solubilizing DCFDA in a trace amount of DMSO and diluting it in excess aqueous medium. The tests were performed as previously reported for the DCFH dye probe[14]. We note that when the DCFH dye was used as a H_2O_2 probe, it suffered very large interferences from most ROS[14]. For instance, the fluorescence increase of the DCFH dye due to ˙OH, ONOO⁻ and ROO˙ was 40, 35 and 4 times that due to H_2O_2, respectively, under the same tetsing conditions as for Table 2.

The DCFDA nanoprobes, in comparison to DCFDA dye, showed a significantly enhanced selectivity towards H_2O_2 over other ROS. Upon exposure to these ROS, DCFDA free dye showed noticeable increases in fluorescence intensity, except for ROO˙. In contrast, the DCFDA nanoprobes exhibited significantly less changes (see Table 2). In the case of ˙OH interference, the slight decrease in the nanoprobe response just reflects the reduced concentration of H_2O_2, by the reaction to produce ˙OH, suggesting negligible interference from ˙OH itself. Notably, ˙OH has the shortest lifetime (nsec or shorter) among all the ROS[36]. Our previous study on ˙OH sensing nanoprobes showed that ˙OH could only be detected at the surface of nanoprobes, but not inside them. This suggests the general principle that nanoparticle matrixes may filter species based on lifetime, thus achieving improved selectivity towards longer-lived ROS. In the case of the HOCl interference, the decrease in the nanoprobe's fluorescence may be because of a pH change in the testing solution, due to HCl production from HOCl[19]. The H_2O_2 response of the DCFDA nanoprobes shows a monotonic pH dependent behavior (Supplementary figure 6)

The ROS like O_2^-, ˙NO, ONOO⁻, HOCl, and ROO˙ (alkylperoxyl radical) are *moderately* unstable ROS molecules, with lifetimes of msec or longer. Exclusion by short lifetime alone may not be sufficient to explain why they are not detected by the nanoprobes. Note that our previous studies have shown that singlet oxygen ($^1O_2$), with a lifetime of only about 2 μsec in aqueous media, can be successfully detected with the same Ormosil-based nanoprobes[37]. It is well known that organic solvents greatly stabilize $^1O_2$, resulting in extension of lifetime[38]. We hypothesize that the relatively hydrophobic Ormosil matrix must offer a similarly favorable environment for lipophilic ROS, such as $^1O_2$ and H_2O_2. On the other hand, it is reasonable to assume that the Ormosil matrix would behave as a hydrophobic energy barrier, reducing the stability of most other polar ROS above. In the presence of ROO˙, neither the free DCFDA dye

nor the nanoprobe exhibited recognizable fluorescence generation, in contrast to the DCFH dye probe[14].

Another important advantage of using DCFDA encapsulated in nanoprobes is the avoidance of unwanted enzymatic interactions. The DCFDA nanoprobes showed no interference from horseradish peroxidase (HRP) but the DCFD free dyes showed significant interference (Table 2). Typically, the ROS assay using DCFH dye is performed in association with HRP[16,17], for faster and more vivid detection, despite the fact that DCFH can be oxidized by HRP alone, without ROS[16,17]. Although this effect is not a significant drawback for general ROS detection, it can cause a very significant error in the H_2O_2-specific quantification. The matrix resistance to HRP interference is due to the large size of the HRP, being too large to penetrate into the Ormosil matrix. The same size exclusion may also eliminate potential confounding interactions from other enzymes or macromolecules. For example, the nanoprobes would be free from unwanted conversion of DCFDA to hydrophilic DCFH by the intracellular esterase, retaining their H_2O_2 selectivity.

Based on the improved H_2O_2 selectivity, H_2O_2 generation from stimulated macrophages, which are well known for oxidative bursts, could be evaluated quantitatively. The surfaces of the DCFDA nanoprobes were engineered for *in vitro* measurement as follows: First, the DCFDA nanoprobes were labeled with a secondary fluorophore, Alexa Fluor 568 succinimidyl ester, because otherwise the nanoprobes are invisible until oxidation (Figure 2-a). Second, a membrane penetrating peptide, cystein terminated TAT peptide (TAT-cys), was conjugated onto the surface of the nanoprobes, so as to deliver them directly to the cytosol[39,40]. As the DCFDA nanoprobe is pH sensitive (Supplementary figure 6), the nanoprobes must be actively delivered to the cytosol, bypassing phagocytotic uptake of macrophages, which is associated with significant acidification[41].

The generation of H_2O_2 from RAW264.7 murine macrophage cells, stimulated by a macrophage stimulant, *N*-formyl-Methiony-*L*-Leucyl-*L*-Phenylalanine (fMLP)[42], was monitored by DCFDA nanoprobes. Two control experiments were performed in parallel, one with the nanoprobes without TAT on the surface, so as to observe the effect of cytosolic delivery, and the other with the TAT-conjugated nanoprobes but without the addition of fMLP, so as to confirm that the response was induced by an oxidative burst. Macrophages without incubation with nanoprobes and without addition of fMLP were used to determine the autofluorescence background of the cells.

The fluorescence intensity changes of the nanoprobes were monitored over 6 hours after addition of fLMP, until the fluorescence was stabilized (Figure 2-b). The TAT conjugated nanoprobes, with stimulation, showed a fast increase of emission intensity for 1 hour, then the rate of increase slowed down until 4 hours, and stabilization occurred later on. The quantity of H_2O_2 detected by the nanoprobes was assessed by comparison with the final product, DCF (from Sigma-Aldrich), applying a 1:1 stoichiometry in the reaction between H_2O_2 and DCFDA dye molecules (overall, $DCFDA+H_2O_2 \rightarrow DCF+H_2O$), based on a literature method[15,43,44] (Supplementary figure 7). Based on the Alexa 568 fluorescence, we estimated the concentration of nanoprobes in the cells to be about 12 mg/mL. This guarantees that there were enough DCFDA nanoprobes inside each cell for a reliable measurement. The H_2O_2 concentration detected by the TAT conjugated nanoprobes, with fMLP stimulation, was equivalent to 18 nM. This result shows that low nM concentrations of H_2O_2 can indeed be successfully detected in live cells by these nanoprobes. The nanoprobes without TAT exhibited a significantly reduced response to H_2O_2, which may imply that the nanoprobe's sensitivity towards H_2O_2 was hindered by the phagocytotic acidification.

In summary, the improved H_2O_2 selectivity of the DCFDA Ormosil nanoprobes is an outcome of a synergistic combination of three different matrix exclusion principles: time barrier, hydrophobic energy barrier, and size barrier. The resultant high specificity is assisted further by negligible dye leaching and by a wide dynamic range, thus enhancing the accuracy and applicability of the measurements. It appears that these DFCDA nanoprobes may provide a powerful chemical detection/imaging tool for investigating biological mechanisms related to H_2O_2, with high spatial and temporal resolution. Similar principles and nanoplatforms may be applied to the determination of other important biochemical species.

Supplementary Material

Refer to Web version on PubMed Central for supplementary material.

Acknowledgments

## References

1. Finkel T, Holbrook NJ. Nature 2000;408(6809):239–247. [PubMed: 11089981]

2. Rhee SG. Science 2006;312:1882–1883. [PubMed: 16809515]

3. Finkel T. Curr opin cell biol 2003;15(2):247–254. [PubMed: 12648682]

4. Babior BM. N EngI J Med 1978;298:659–668.

5. Oren R, Farnham AE, Saito K, Milofsky E, Karnovsky ML. J Cell Biol 1963;17(3):487–501. [PubMed: 13940299]

6. Karnovsky, ML.; Lazdins, J.; Simmons, SR. Mononuclear phagocytes in immunity, infection and pathology. Blackwell, Oxford: 1975. p. 423-439.

7. Nathan CF, Root RK. J Exp Med 1977;146(6):1648–1662. [PubMed: 925614]

8. Niethammer P, Grabher C, Look AT, Mitchison TJ. Nature 2009;459(18):996–1000. [PubMed: 19494811]

9. Dröge W. Physiol rev 2002;82(1):47–95. [PubMed: 11773609]

10. Colavitti R, Pani G, Bedogni B, et al. J Biol Chem 2002;277(5):3101–3108. [PubMed: 11719508]

11. Pryor, WA. Free radicals in biology. Vol. I. Academic Press Incorporated; New York, NY: 1976.

12. Grisham, MB. Reactive metabolites of oxygen and nitrogen in biology and medicine. RG Landes Co; Austin: 1992.

13. Eberhardt, MK. Reactive oxygen metabolites: chemistry and medical consequences. CRC press; Boca Raton, FL: 2000.

14. Setsukinai K, Urano Y, Kakinuma K, Majima HJ, Nagano T. J Biol Chem 2003;278(5):3170–3175. [PubMed: 12419811]

15. Royall JA, Ischiropoulos H. Arch Biochem Biophys 1993;302(2):348–355. [PubMed: 8387741]

16. Keston AS, Brandt R. Anal Biochem 1965;11(1):1–5. [PubMed: 14328641]

17. LeBel CP, Ischiropoulos H, Bondy SC. Chem Res Toxicol 1992;5(2):227–231. [PubMed: 1322737]

18. Keller A, Mohamed A, Dröse S, et al. Free Radical Res 2004;38(12):1257–1267. [PubMed: 15763950]

19. Afri M, Frimer AA, Cohen Y. Chem phys lipids 2004;131(1):123–133. [PubMed: 15210370]

20. Clark HA, Barker SLR, Brasuel M, et al. Sensor Actuator: B Chemical 1998;51(1–3):12–16.

21. Xu H, Buck S, Kopelman R, et al. Israel J Chem 2004;44(1):317–337.

22. Koo, LY.; Monson, E.; Brasuel, M.; Philbert, MA.; Kopelman, R. Biomedical Photonics Handbook. 2. Vo-Dinh, T., editor. CRC press; 2009. in press

23. Koo LY, Smith R, Kopelman R. Annu Rev Anal Chem 2009;2:57–76. [PubMed: 20098636]

24. Gong X, Li Q, Tang B, et al. Electrophoresis 2009;30:1983–1990. [PubMed: 19517439]

25. Dickinson BC, Chang CJ. J Am Chem Soc 2008;130:9638–9639. [PubMed: 18605728]

26. Maeda H, Fukuyasu Y, Yoshida S, et al. Angew Chem Int Ed 2004;43:2389–2391.

27. Lee D, Khaja S, Velasquez-Castano JC, et al. Nat Mater 2007;6(10):765–769. [PubMed: 17704780]

28. Lee D, Erigala VR, Dasari M, et al. Int J Nanomed 2008;3:471–476.

29. Rauhut MM, Bollyky LJ, Roberts BG, et al. J Am Chem Soc 1967;89(25):6515–6522.

30. Kim SH, Kim B, Yadavalli VK, Pishko MV. Anal Chem 2005;77(21):6828–6833. [PubMed: 16255579]

31. Poulsen AK, Scharff-Poulsen AM, Olsen LF. Anal biochem 2007;366(1):29–36. [PubMed: 17498639]

32. Hah HJ, Kim JS, Jeon BJ, Koo SM, Lee YE. Chem Comm 2003:1712–1713.

33. Koo YL, Cao Y, Kopelman R, et al. Anal Chem 2004;76(9):2498–2505. [PubMed: 15117189]

34. Pinto RC, Neufeld RJ, Ribeiro AJ, Veiga F. Nanomed Nanotechnol Biol Med 2006;2(1):8–21.

35. Tyner KM, Kopelman R, Philbert MA. Biophys J 2007;93(4):1163–1174. [PubMed: 17513359]

36. King M, Kopelman R. Sensor Actuator: B 2003;90(1–3):76–81.

37. Cao Y, Koo YL, Koo SM, Kopelman R. Photochem Photobiol 2005;81(6):1489–1498. [PubMed: 16107183]

38. Ogilby RR, Foote CS. J Am Chem Soc 1983;105:3423–3430.

39. Fawell S, Seery J, Daikh Y, et al. P Natl Acad Sci 1994;91(2):664–668.

40. Webster A, Compton SJ, Aylott JW. Analyst 2005;130(2):163–170. [PubMed: 15665969]

41. Nyberg K, Johansson U, Rundquist I, Camner P. Exp lung res 1989;15(4):499–510. [PubMed: 2767002]

42. Snyderman R, Fundman EJ. I Immunol 1980;124(6):2754–2757.

43. Esposti MD, McLennan H. FEBS Letters 1998;430:338–342. [PubMed: 9688567]

44. Black MJ, Brandt RB. Anal Biochem 1974;58:246–254. [PubMed: 4825377]
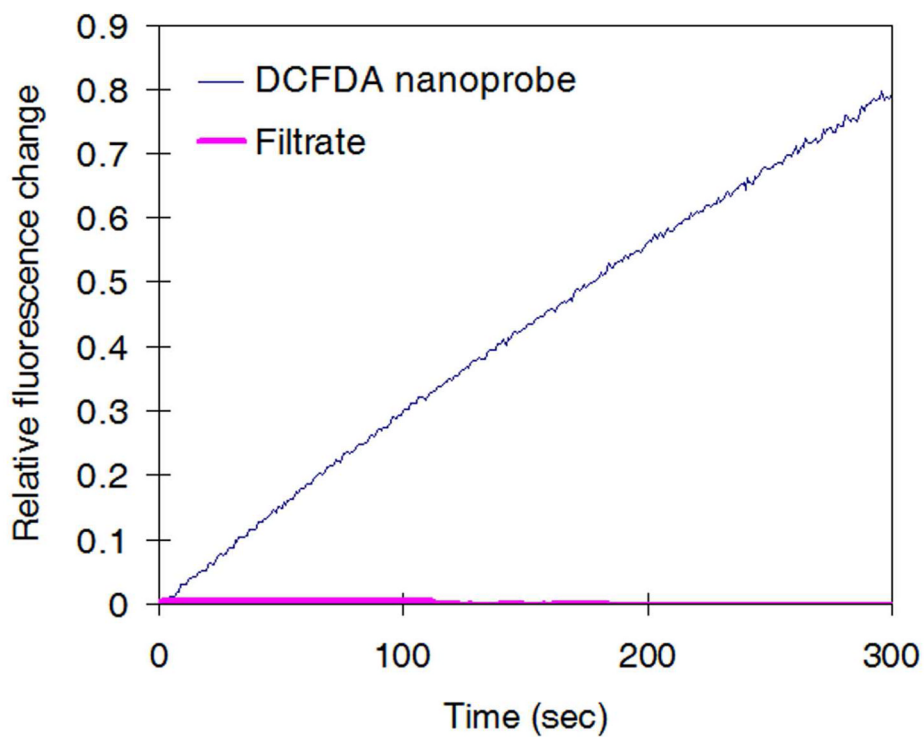
Figure 1.
Negligible dye leaching from DCFDA nanoprobes. Filtrate of DCFDA nanoprobes did not respond to H_2O_2, indicating that the reaction between DCFDA dye and H_2O_2 was confined to the inside of the nanoparticle matrix. Note that the change of filtrate's fluorescence values are so small that they are barely visible in the chart. This Figure validates the hypothesis of induced selectivity by nanoencapsulation.
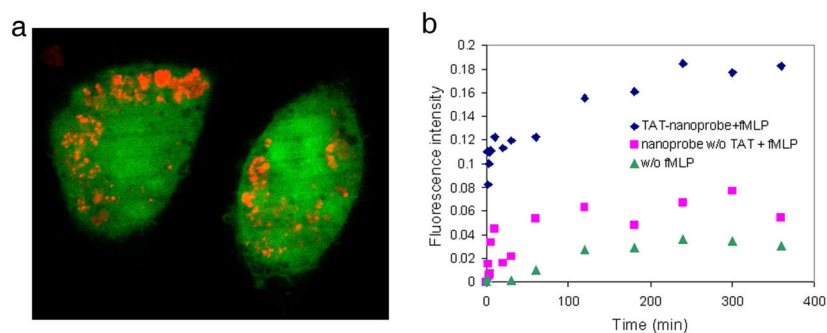
Figure 2.
In vitro H_2O_2 detection performed with DCFDA nanoprobes. a) Confocal image showing cellular uptake of DCFDA nanoprobes. The nanoprobes were incubated with RAW264.7 macrophage cells overnight. The nanoprobes were delivered to the cytosol by the TAT peptide function. The cells were stained by Calcein-AM (green colored, ex: 488 nm, em: 525 nm) and the nanoprobes were visualized by a secondary label, Alexa 568 (red colored, ex: 568 nm, em: 600 nm). b) Fluorescence increase over time due to H_2O_2 generation from macrophages upon stimulation with fMLP: TAT-conjugated nanoprobes (◆), control without TAT (■), and control without stimulation (▲). The DCFDA nanoprobes showed a significantly larger increase of fluorescence from stimulated cells than from the control (caused by auto-oxidation or natural H_2O_2 generation).
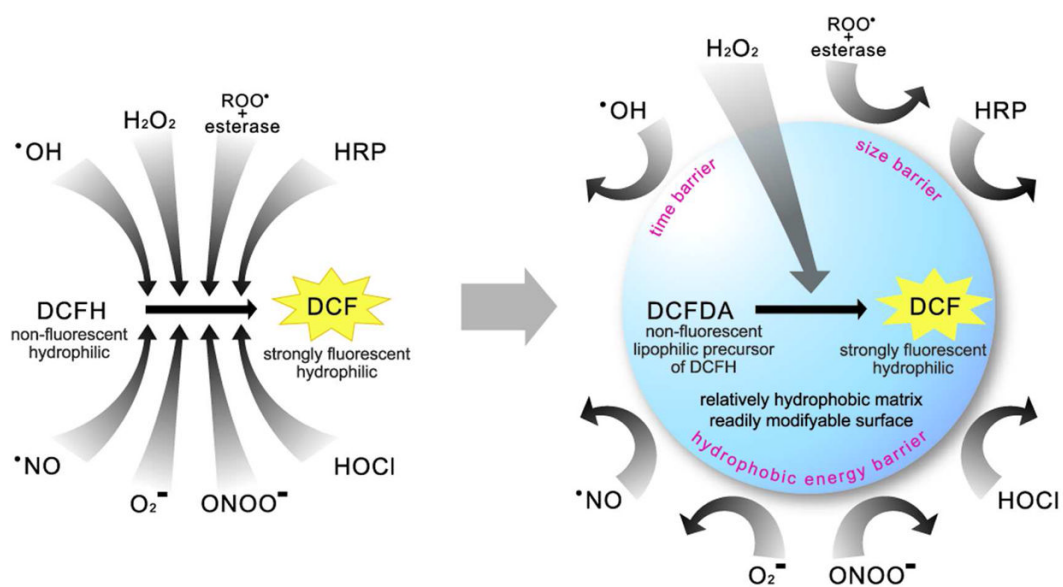
Scheme 1.
Schematic representation of induced H_2O_2 selectivity by encapsulating DCFDA into relatively hydrophobic Ormosil nanoparticles. The left scheme shows that DCFH (activated form) can be oxidized by a variety of interferents. The right scheme shows that a relatively hydrophobic nanoparticle matrix encapsulating DCFDA (precursor form) can filter the interferences, thus only allowing penetration of H_2O_2, resulting in high selectivity towards this specific analyte.

Table 1

The DCFDA nanoprobes' H_2O_2 sensitivity vs concentration. DCFDA nanoprobes show a fluorescence generation that increases monotonically with the H_2O_2 concentration.

H_2O_2 concentration	Fluorescence increase over 5 minutes
87 µM	5045 ± 585 %
8.7 µM	543 ± 79 %
870 nM	94 ± 17 %
87 nM	41± 5 %
8.7 nM	17 ± 6 %
0 nM	2 ± 2%

Table 2

DCFDA nanoprobe resistance to interferences from other ROS and HRP. The fluorescence generation upon introduction of various ROS interferents is compared between a solubilized DCFDA free dye solution (dissolved in a trace amount of DMSO and then diluted in an excess amount of aqueous media) and the DCFDA nanoprobes solution. Note, however, that the activated free dye, DCFH, is much more sensitive to ROO$^\cdot$ (in Supplementary figure 8-f).

Interfering ROS	Fluorescence increase over 5 minutes	
	DCFDA free dye	Nanoprobe
$^{\cdot}$OH[a]	24.1 ± 0.3 %	$- 6.8 \pm 0.0$ %
O_2^{-}[b]	53.3 ± 4.2 %	0.0 ± 0.9 %
$^{\cdot}$NO[c]	26.6 ± 3.3 %	$- 0.4 \pm 0.9$ %
$ONOO^{-}$[d]	199.4 ± 17.9 %	15.3 ± 2.4 %
HOCl[e]	55.2 ± 6.0 %	$- 26.8 \pm 6.1$ %
ROO$^{\cdot}$[f]	0.0 ± 0.8 %	0.0 ± 0.1 %
HRP[g]	556.5 ± 16.8 %	1.9 ± 0.1 %

[a] Generated from Fenton reaction (Fe^{2+} + H_2O_2), ferrous chlorate (final 1 μM) and H_2O_2 (final 8.7 μM). Note that the fluorescence increase here results from both $^{\cdot}$OH radical and H_2O_2.

[b] Generated by ionization of KO_2 in aqueous medium, (final 100 μM O_2^{-})

[c] From $^{\cdot}$NO saturated stock solution, (final 20 μM $^{\cdot}$NO)

[d] From commercially available $ONOO^{-}$ solution (final 3.5 μM, from Cayman Chemicals)

[e] Generation from ionization of NaOCl (final 3 μM $^{-}$OCl)

[f] Generated by thermolysis of 2,2-Azobis(2-amidinopropane)dihydrochloride in 37 °C (final 100 μM ROO$^{\cdot}$)

[g] HRP was added into the solution (final 10 μM HRP).